Sarcouncil Journal of Engineering and Computer Sciences

ISSN(Online): 2945-3585

Volume- 04| Issue- 09| 2025

Research Article **Received:** 25-07-2025| **Accepted:** 15-08-2025 | **Published:** 08-09-2025

Study of Charge Trapping and De-Trapping Phenomena through Vacuum Charge Measurements and Photoinduced Discharge in Polymeric Thin Films for Energy Storage

Alwan Flayyih Hussein

Independent researcher, Iraq

Abstract: This study investigates charge trapping and de-trapping phenomena in polymeric thin films, specifically biaxially oriented polypropylene (BOPP), for energy storage applications. Using the LIMM-PSD measurement system, electrical conduction mechanisms were analyzed during polarization and depolarization phases, highlighting the predominance of space-charge-limited conduction (SCLC) under specific electric field ranges. A charge injection limit of 126 kV/mm was identified, marking the transition from ohmic conduction to transport dominated by space-charge effects. Charge trapping is strongly influenced by interfacial phenomena at the conductor-insulator boundaries, where the polymer's band structure determines the potential barrier for carrier injection. Surface states formed at these interfaces facilitate hole injection, whereas electron injection is constrained by blocking contacts, occurring only under high fields or via tunneling. Bulk conduction is governed by the density and energy depth of trapping states, with shallow traps favoring negative charge accumulation. Photoinduced discharge (PSD) analysis, correlated with UV-visible absorption spectra, revealed the presence of extrinsic entities affecting charge dynamics. Two main excitation bands were observed: S1 excitons around 3.1 eV, potentially linked to transition metal ions and free charge generation via the Auger effect, and high-energy S2 excitons around 6.2 eV, associated with chemical additives such as phenolic antioxidants, which can release electrons under residual fields. Although PSD irradiation did not produce significant changes in sample charge density, the study enabled identification of chromophoric species influencing trapping behavior. Extending this research to other nonpolar, light-absorbing polymers could improve understanding of charge trapping and release mechanisms in polymer-based energy storage materials.

Keywords: Trapping, rapping phenomena, charge measurements, photoinduced discharge, polymeric thin films, energy storage.

INTRODUCTION

Electrical conduction mechanisms, associated with charge trapping and detrapping phenomena, were experimentally studied on thin BOPP samples using the LIMM-PSD measuring device. The acquisition of currents during the polarization and depolarization phases made it possible to identify various electrical conduction mechanisms, among which the SCLC characteristic particularly stands out for the range of applied electric fields. The identification of a charge injection limit at 126 kV/mm makes it possible to define the critical point where ohmic conduction gives way to transport conditioned by the formation of space charge.

Charge trapping within the material, in response to the direct application of an electric field using conductive electrodes, initially relies on phenomena occurring at the interfaces between the conductor and the insulator. The charge injection barrier is mainly determined by the polymer, whose band energy distribution conditions the height of the potential barrier. (Mayerhöfer, T. G. *et al*., 2020)

The formation of an electrical double layer at the interface can explain the creation of surface states favorable to hole injection. In contrast, electron injection is constrained by the blocking contact, which only allows the passage of carriers under specific conditions, such as a high electric field or a reduction in the barrier width, favoring the tunneling effect. Conduction beyond the first few micrometers of depth is subject, among other factors, to the density of trapping states and their energy depth, thus generating a preponderance of negative charge due to higher densities of shallow traps that favor bulk transport

RESEARCH METHOD

The current density versus applied field characteristic, as illustrated in Figure III.1-2, reveals two distinct conduction regions.

***Corresponding Author:** Alwan Flayyih Hussein

DOI- https://doi.org/10.5281/zenodo.17080418

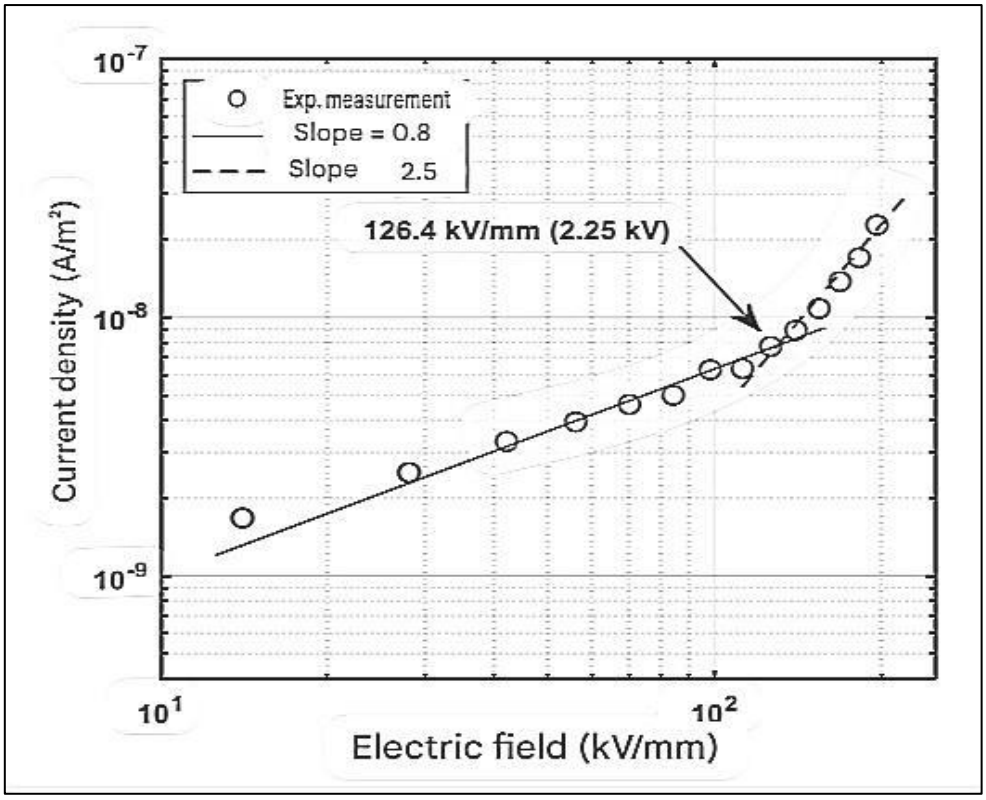

Graphs: 1

The first region exhibits linear behavior with a slope approximately equal to 1, indicating the predominance of the ohmic conduction mechanism. In this region, the density of injected carriers is negligible compared to the intrinsic dipolar orientation of the material.

When external fields greater than 126 kV/mm are applied, a notable transition occurs, marked by an increase in current density and characterized by linear behavior with a slope greater than 2.5. This second region reflects a conduction regime limited by trap occupancy.

In this phase, injected charges become predominant, occupying the available traps and thus contributing to the increase in conduction current. It is worth noting that the linear approximation of this region, with a slope between 2 and 4, may reflect an energy distribution of traps at different energy levels. (Xu, R. *et al*., 2021)

The regime change observed near 126 kV/mm, as illustrated in Figure III.1-2, could be attributed to the presence of the charge injection boundary, given the absence of any other region in the applied field range. Similar investigations have been carried out on BOPP films with nominal thicknesses of 7.6 µm and 12.5 µm, highlighting the transition point between ohmic conduction and the space-charge-limited region, located beyond 100 kV/mm , At higher electric fields, for example, between 200 kV/mm and 450 kV/mm, a new region emerges beyond 380 kV/mm, where all available traps are occupied .

The identification of the different areas of the J-E characteristic suggests the preponderance of the SCLC (Space Charge Limited Conduction) type of conduction mechanism. The SCLC conduction model can be illuminated by considering other mechanisms such as ohmic conduction at very low fields and the effect of Schottky injection as the field gradually increases As the field reaches high levels, charge trapping takes over, thus justifying the adoption of the jump conduction model .

With this in mind, it is essential to note that charge conduction and trapping depend not only on phenomena occurring within the insulator, but also on interactions with the electrodes used. Indeed, the appearance and displacement of charges are partly determined by the emissive capacity of each material, the mechanisms operating at the interfaces, as well as those occurring within the bulk of the material.

In the context of the metal-insulator-metal (MIM) configuration, it becomes imperative to examine the behavior of charges at the interfaces, focusing on the analysis of the potential barrier created at these contact points The gold-BOPP-gold

Publisher: SARC Publisher

configuration is known to be a blocking contact due to the difference in their energy levels. Gold has a work function om estimated at 5.3 eV which is greater than the energy difference between the BOPP Fermi level, denoted Er, and the vacuum level, estimated at 2.59 eV .

Therefore, when these components are separated as shown in Figure 1(a), electrons are unlikely to be emitted from the metal to the insulator due to the energy value ' required to emit electrons at the LUMO level of the insulator ,The value + corresponds to the energy required to allow the passage of holes ,When the materials are brought into close contact with each other, as is the case when gold electrodes are evaporated onto the polymer, electrons from the HOMO level of BOPP move toward the metal to adjust the Fermi levels in a continuum, thus reducing the AEF energy difference.

between the Fermi levels of the materials. As a result, negative charges are transferred to the metal surface, while positive charges (holes) emerge on the insulator surface, creating surface states. This configuration is commonly referred to as an electric double layer , Figure 1 (b) illustrates the contact between the two materials and highlights the reduction in the electron injection barrier. The positively charged surface states facilitate the injection of holes from the metal to the insulator, while the electrons available at the LUMO level of the insulator can easily flow from the BOPP to the metal. (Takada, T. *et al*., 2022).

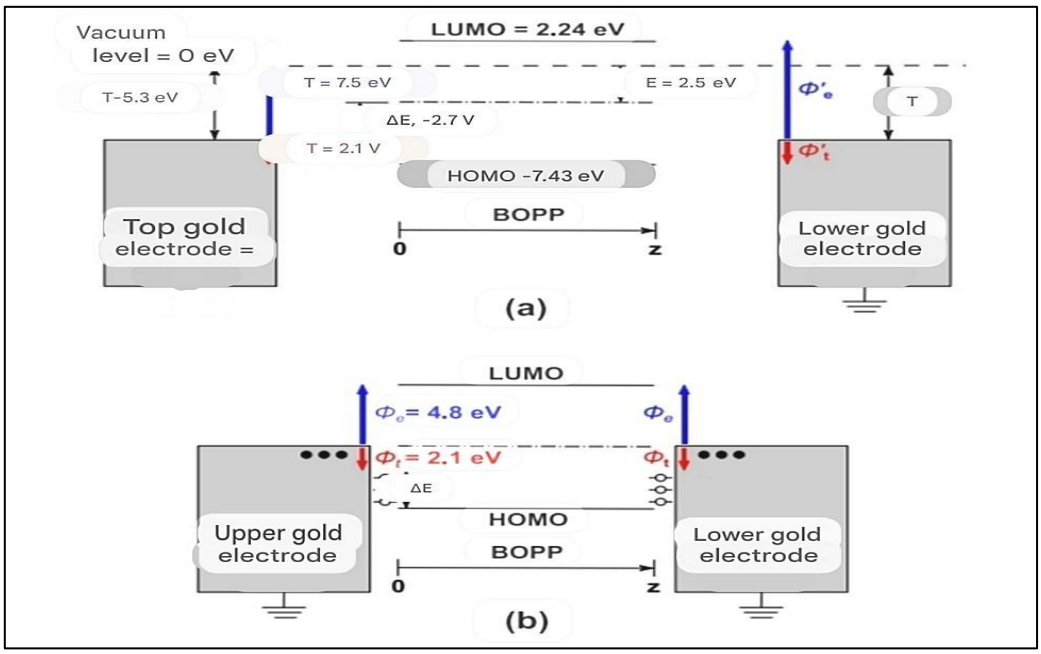

Figure 1. Theoretical energy diagram of the gold-BOPP-gold configuration before contact (a) and after contact (b).

When a potential difference is applied to the evaporated electrodes, the potential barrier characteristics at the interfaces vary in terms of height and width, When a positive bias is applied to the top electrode, the interface at the anode exhibits quasi-ohmic behavior for hole injection, since the metal is able to supply holes to the insulator.

In contrast, the cathode interface acts almost as a blocking contact for electron injection, with a high electron injection barrier, as shown in Figure 2(a). This implies that, under electric field conditions greater than the carrier injection limit, positive charges are injected from the top electrode to the insulator, using the positively charged surface states. Simultaneously, electrons can be easily extracted from the BOPP to the top electrode.

The gradual formation of the positive space charge at proximity to the top electrode, as identified in Figures IV.2-1 and IV.2-2, may therefore result from the ability of holes to cross the injection barrier at electric fields above 126 kV/mm, and to tunnel through them at even higher fields. As for the cathode, the potential barrier limits the injection of electrons from the metal to the insulator.

When the polarity of the power source is reversed, electronic conduction is then restricted by the interface located at the top electrode. The height and width of the injection barrier therefore play a

Publisher: SARC Publisher

determining role in regulating the flow of electrons from the metal to the insulator, as illustrated in Figure 2 (b). Electrons that have successfully overcome this barrier can recombine with previously accumulated holes, resulting in a reduction in the positive charge density during the early stages of negative voltage (Liu, H. *et al*., 2021).

When negative-polarity fields reach high levels, more electrons can be generated due to the thermoelectronic effect and tunneling. This tunneling is aided not only by the applied electric field but also by the previously accumulated positive space charge, which can reduce the width of the injection barrier .

In this configuration, some electrons remain trapped near the top electrode, while others can be transported through the insulator in search of the bottom electrode.

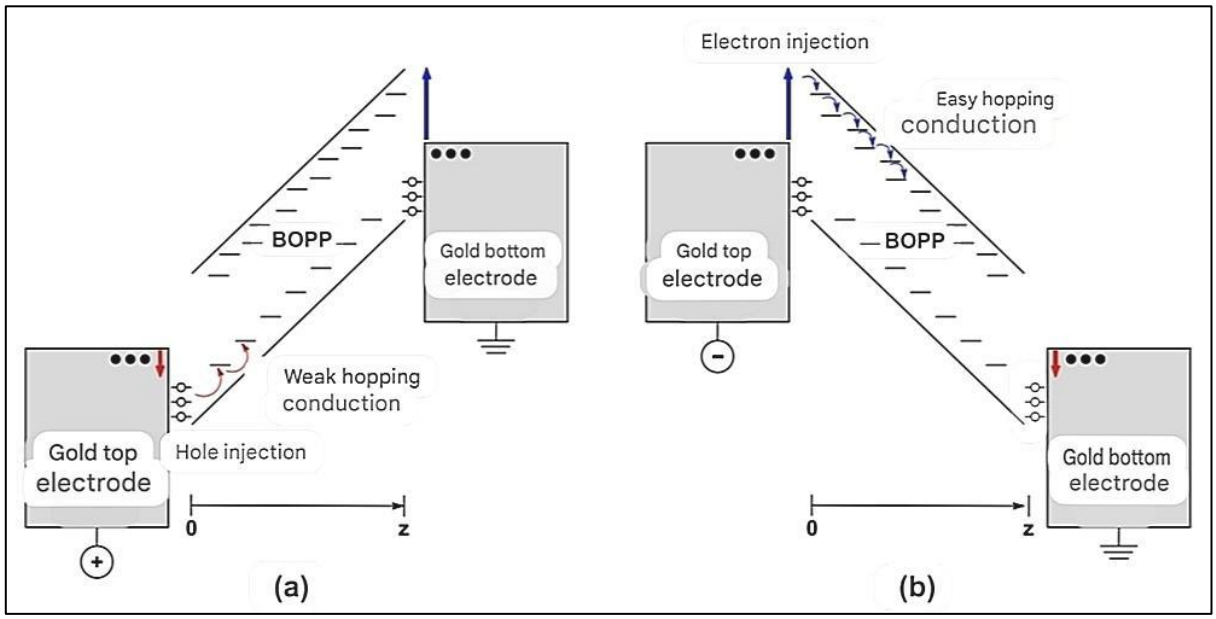

Figure 2. Theoretical energy diagram of the gold-BOPP-gold configuration for a positive polarity field (a) and a negative polarity field (b) at the upper electrode.

Figure 2 reveals substantial differences in the conduction of holes and electrons near the electrode. In particular, limited hole transport is observed in the bulk, attributable to the presence of deep.

In contrast, electron transport is facilitated due to the presence of shallow and more frequent traps. The volume transport of injected charges is intrinsically linked to the characteristics of the traps, both in terms of energy and density. Indeed, shallow localized states favor conduction phenomena in polymers, while deep traps are closely associated with trapping and space charge . (Yuan, M. *et al*., 2020)

Molecular simulations performed using the DFT method revealed that, in the case of PP, the conduction mechanisms of electrons and holes exhibit marked dissimilarities , the molecular orbitals corresponding to the LUMO level, which are associated with electron traps, are localized on the surface of the molecular chains This observation suggests that an injected electron tends to move mainly outside the polymer chains, particularly into the interstitial spaces between these chains, where it can be easily accelerated. In contrast, molecular orbitals located at the HOMO level are distributed within the chains themselves.

This means that valence electrons have more interactions with the molecular chains, and potentially with any defects that may be present there. In other words, when a hole is introduced into a neutral PP, it will be mainly attracted to the chemical defects present along the chain backbone. In contrast, when an electron is added, it will be mainly repelled by the macromolecular chains and will settle between these chains, in the amorphous regions.

Experimental studies have corroborated the conclusions of the simulations, highlighting a distinction in the distribution of traps for holes and electrons within the polypropylene-based material To illustrate this, surface potential behavior analysis was used to establish that deep traps for holes and electrons within PP exhibit similarities

Publisher: SARC Publisher

in their respective density and energy. (Yuryevna Ridzel, O. *et al*., 2022)

However, the density of shallow traps for electrons is found to be up to five orders of magnitude higher than that of shallow traps for holes ,This observation could indicate a greater ease of transport of electrons out of molecular chains, through shallow localized states. Another investigation presented an algorithm to calculate charge decay, which was used to study the energy distribution of traps and their density ,The results of this study revealed that deep traps for holes display a higher density than their counterparts for electrons. Therefore, it is conceivable that the accumulation of positive charges within traps deep traps is more likely than their transport through shallow traps. A distinct approach suggests that the energy of traps for electrons is shallower than that for holes .

Indeed, the former are in the energy range of 0.82 eV to 0.93 eV, while the latter occupy a range of 0.92 eV to 0.97 eV. This body of evidence therefore suggests that traps for holes vary in depth, with some being deeper than others, while traps for electrons are shallower and display a higher density. As a result, hole transport is limited, while electron transport is favored In the BOPP samples studied in this study, charge accumulation near the top electrode can be summarized as follows: when a positive-polarity electric field is applied, it is easy to introduce positive charges, but their mobility is restricted due to the small number of shallow traps for holes.

The existence of deep traps hinders their movement, thus causing the formation of a positive space charge in the first few micrometers of the material's thickness. On the other hand, when the polarity of the applied electric field is reversed, negative charges are injected beyond the injection barrier and can easily circulate through the shallow traps for electrons, which have a higher density than the traps for holes Deep electron traps have reduced energy, which promotes extensive electron migration throughout the material, thus explaining the formation of a negative space charge extending to a depth of 6 µm.

Two sources of negative charges deserve consideration. The first source assumes the injection of electrons toward the cathode. In this scenario, it is postulated that the density of shallow electron traps is high enough to facilitate electronic conduction. The second source envisages the presence of bulk ionizable species that, under the effect of the electric field, release carriers migrating toward regions of opposite charge, thus creating a form of heterocharge. Recently studied ionizable impurities within polypropylene include metal residues from polymerization processes, such as titanium (Ti) or magnesium (Mg), as well as impurities such as iron from manufacturing tools , It has been established that these metallic impurities present in polymers generate a large number of polar functional groups, including carbonyl (C=O), hydroxyl (OH), vinyl, and conjugated double bonds. These polar impurities create charge carriers under the influence of the electric field, thus promoting conduction phenomena.

The carriers thus generated can then migrate and be captured by bulk trapping sites, which has the effect of distorting the local electric field With the progressive increase of the positive external field, the gradual formation of the positive space charge near the upper electrode hinders the exit of the negative charges that had been transported towards the anode, thus reinforcing their accumulation in volume When considering a protocol starting with negative polarity fields and ending with positive polarity, as shown in Figure III.2-2, the dynamics remain very similar.

Consistent with previous explanations, the mechanisms operating at the upper interface initially allow the transfer of electrons from the electrode to the insulator under negative polarity, thus generating the formation of negative space charge near the cathode. Subsequently, under positive polarity, these electrons are emitted in the opposite direction, thus freeing up space for holes to restore space charge balance by accumulating near the upper electrode Regardless of the field polarity applied at the beginning of the protocol, the predominance of negative space charge in terms of spatial depth remains evident. This result can also be amplified by the effects of the edges of the serrated electrode, which frequently induce an alteration of the electric field. Consistent with electrostatic simulations, the use of serrated electrodes generates regions where the electric field is increased up to five times its average magnitude as demonstrated in Figure 3. This field intensification near the edges of the upper electrode can increase the injection of both positive and negative charges, depending on the polarity of the field applied to the serrated electrode. The more abundantly the charges are

Publisher: SARC Publisher

injected, the more likely they are to be transported into the volume. (Ran, Z. Y. *et al*., 2021)

However, due to the disparities in energy and density of the hole and electron traps, it is the latter that demonstrate an increased propensity to move easily under the influence of the field.

RESEARCH RESULTS

The light radiation irradiating the studied samples has the ability to interact directly with areas not covered by the metal electrode or with the serrated gold layer. Consequently, the PSD current spectra can result from phenomena operating in these two regions, unlike to space charge maps, which focus exclusively on thermal interactions with the metal-insulator or metal-ITO-insulator zones.

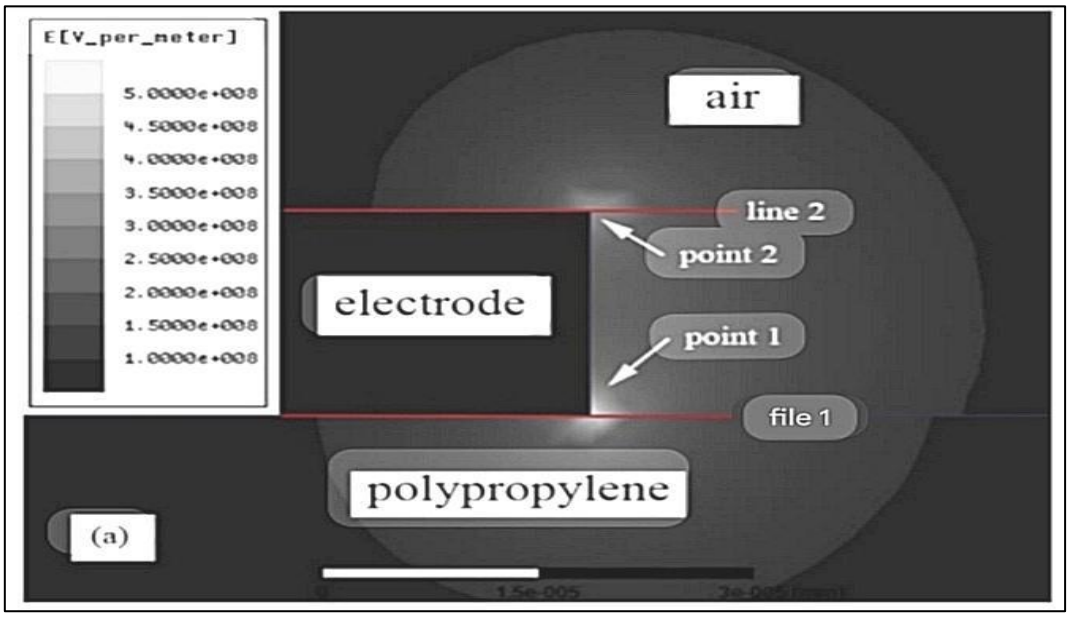

Figure 3. Electric field distribution near the edge of the finger electrode (or serrated electrode) when a finger-Au - solid Au electrode configuration is under 100 V

Direct photon absorption by BOPP arises from the presence of chromophoric components in its molecular structure Theoretically, based on the absorption characteristics of isolated polyolefins, it is believed that they should not contain chromophores absorbing or emitting in the UV-visible range. However, it is important to note that chemical and physical defects, resulting from material degradation or manufacturing processes, invariably remain and are known to absorb in more or less defined absorption ranges. (Ohki, Y. *et al*., 2010)

These defects include unsaturated species tightly bound to the polymer chain, referred to as intrinsic species, as well as those resulting from the presence of additives or impurities, referred to as extrinsic species Figure 4 (a) presents the UV-vis absorption spectra of an unmetallized sample as initially received, highlighting the impact of continuous exposure to 200 nm light radiation for a duration of 180 minutes.

The untreated sample reveals a distinct and significant absorption peak at approximately 6.2 eV (200 nm), a peak located at the edge of the growing region at 5.3 eV (238 nm), and a lower-intensity peak at 4.4 eV (280 nm). After 180 minutes of irradiation, the absorption of the high-energy peak decreases by approximately 20%. In addition, the absorption range between 3.2 eV and 5.1 eV shows an increase in its absorption intensity.

These observations are consistent with the findings of Ho et al., who demonstrated the presence of antioxidants, such as than Irganox 1010 in BOPP, having a predominant absorption capacity in the UV spectrum and inducing the formation of by-products, including olefinic ketones, It should be noted that in the polyolefin industry, primary antioxidants, such as Irganox 1076 or Irganox 1010, are commonly incorporated into PP during manufacturing processes to improve the material's resistance to oxidation.

However, it is precisely this interaction with oxygen molecules that constitutes the main degradation pathway for sterically hindered phenols. In this context, phenolic hydrogens are donated to radicals from the polymer, leading to the formation of quinone-like structures

Publisher: SARC Publisher

,Photodegradation byproducts identified for these antioxidants include the molecule 2,6-di-tert-butyl-p-benzoquinone (2,6-DTB-PBQ) and stilbenequinone, which generally exhibit absorption peaks at approximately 3.7 eV and 4.9 eV . (Uehara, H. *et al*., 2021)

Figure 4(b) provides a representation of the light penetration depth of the BOPP film, calculated from the transmission spectrum. In an energy range from 2 eV to 5.1 eV, light is able to travel a distance of 12 to 16 µm. At higher energies, the distance traveled by light decreases, reaching a minimum of 7 µm, which remains relatively deep.

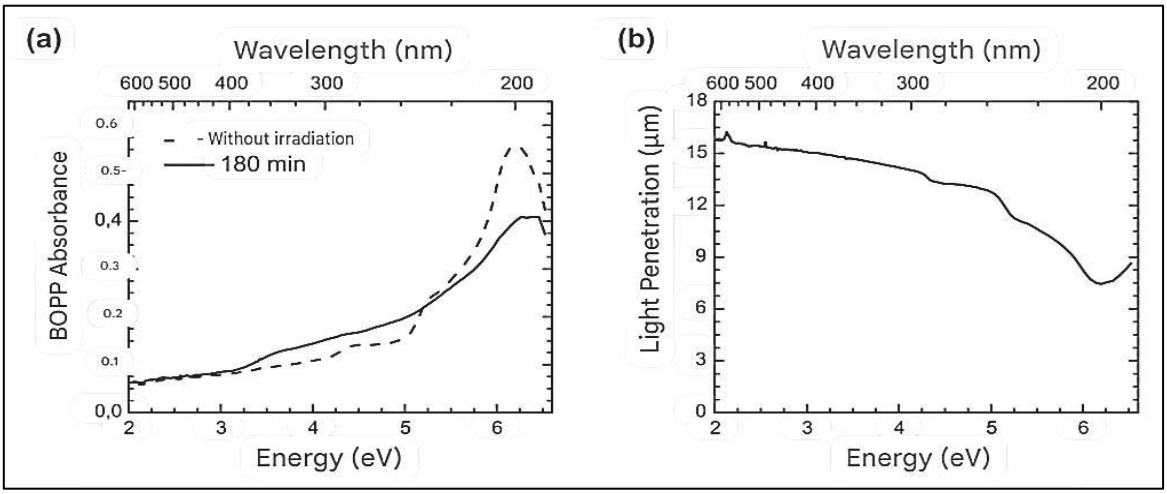

Figure 4. UV-vis absorption spectra of a BOPP film before and after 200 nm light irradiation (a). Light penetration depth in a BOPP film (b).

When an ITO layer is placed on the samples, part of the spectrum is absorbed by the layer and another part is transmitted, as shown in Figure 5. Light excitations with energies greater than 5 eV are absorbed by the ITO layer and do not interact with the polymer. In On the other hand, lower-energy radiation will be able to pass through the conductive layer, ranging from a low transmission value of 5% to nearly 75% for energies between 2 eV and 3.1 eV.

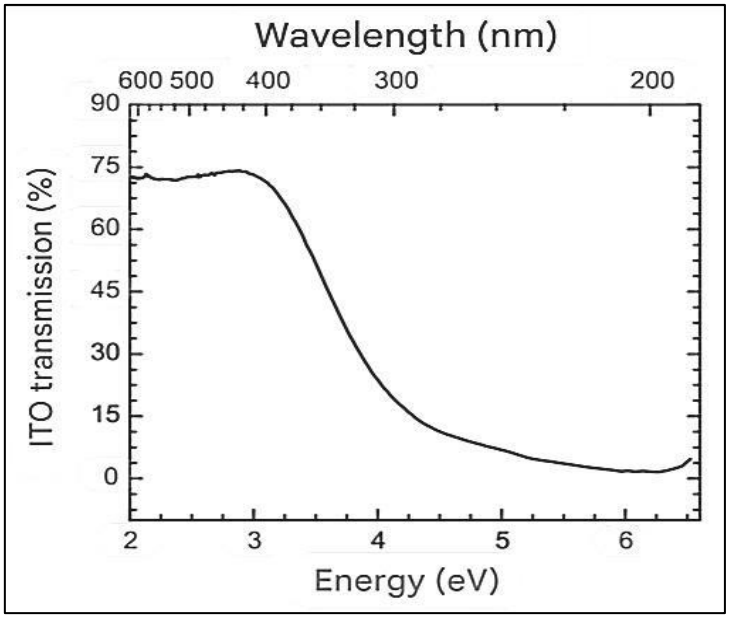

Figure 5. Transmission spectrum of an ITO layer placed on a BOPP film.

The PSD spectra reveal the presence of current peaks at specific energy levels, which can be correlated with the absorption bands of the material. The values obtained for the BOPP samples, whether or not coated with an ITO layer, are summarized in Table 1 The peaks at 3.1 eV and 3.3 eV do not directly correspond to the absorption bands observed in UV-vis spectroscopy measurements.

Publisher: SARC Publisher

However, the use of other techniques, such as derivative spectroscopy, provides results indicating the presence of bands at 3.12 eV and 3.54 eV (S1), possibly associated with transition metal ions such as Fe3+ ,The peak at 4.8 eV is observable in samples coated with an ITO layer, and its value is close to the band corresponding to the non-bonding n-transitions of carbonyl groups, identified between 4.4 eV and 4.7 eV .

Finally, the most pronounced peak, located at an energy of 5.9 eV, can be associated with a broader absorption band with a maximum at 6.2 eV (S2), containing the (l-l*) transitions of isolated or unsaturated carbonyl groups isolated diene double bonds and/or sterically hindered phenolic antioxidants In particular, it is worth noting the presence of Irganox 1010 in the BOPP film, which demonstrated the presence of a band gap at 5.4 eV from electron reflection energy loss spectra ,Indeed, phenyl ketone groups, such as those of antioxidants, manifest optically above 5.2 eV . (Teyssedre, G. *et al*., 2021).

Table 1. Relationship between PSD and absorption current peaks optical

Pics PSD (eV)		Optical absorption (eV)		
Energy (eV)	Electrode Type	This study	Other studies	Excited level
3.1 eV - low	Gold - serrated	-	3.1 - 3.5 [71]	S1
3.3 eV - low	ITO - disk	-		
4.8 eV - low	Gold - serrated ITO - disk	4.4	4.7 [71]	-
5.9 eV - pronounced	Gold - serrated	6.2	5.3 - 5.4 [71] 5.2 - 6.2 [72] 6.2 [103]	S2

Molecular dynamics calculations typically present the density of states and energy levels of isolated polypropylene molecules, without considering the impact of additives, such as antioxidants, which significantly modify the energy distribution within these materials.

Traditionally, PP is associated with a relatively wide band gap of approximately 9.6 eV However, experimental studies have revealed that polyolefin-type polymers, such as PP, actually exhibit a band gap of approximately 7 eV ,This observation constitutes a considerable difference from the predictions of quantum models.

In fact, when molecules external to the polymer chain, such as phenolic antioxidants, are considered, the energy levels undergo changes due to charge redistribution and, consequently, alterations in molecular orbitals.

For example, the addition of a phenolic antioxidant to polyethylene leads to a concentration of the molecular orbitals of the LUMO and HOMO levels near the antioxidant, instead of their usual distribution between the PE molecules, as occurs when only the polymer chain is considered. This redistribution results in a decrease in the LUMO level of 2.5 eV and an increase in the HOMO level of 1.6 eV, thus creating deep traps for electrons and holes.

It is worth noting that the incorporation of Irganox 1010 into PP could generate a similar effect on the energy scheme of the material, inducing the formation of deep traps and potentially reducing the band gap width ,Starting from the energy diagrams established by Xu et al. and Liu et al., which indicate a band gap of 9.6 eV and taking into account both the transitions associated with the transition metal ions (S1), the excited levels generated by the presence of the antioxidant (S2) as well as the absorption bands listed in Table 1, it is possible to Formulate a diagram of the electronic optical absorption transitions for BOPP, as presented in Figure 6.

Publisher: SARC Publisher

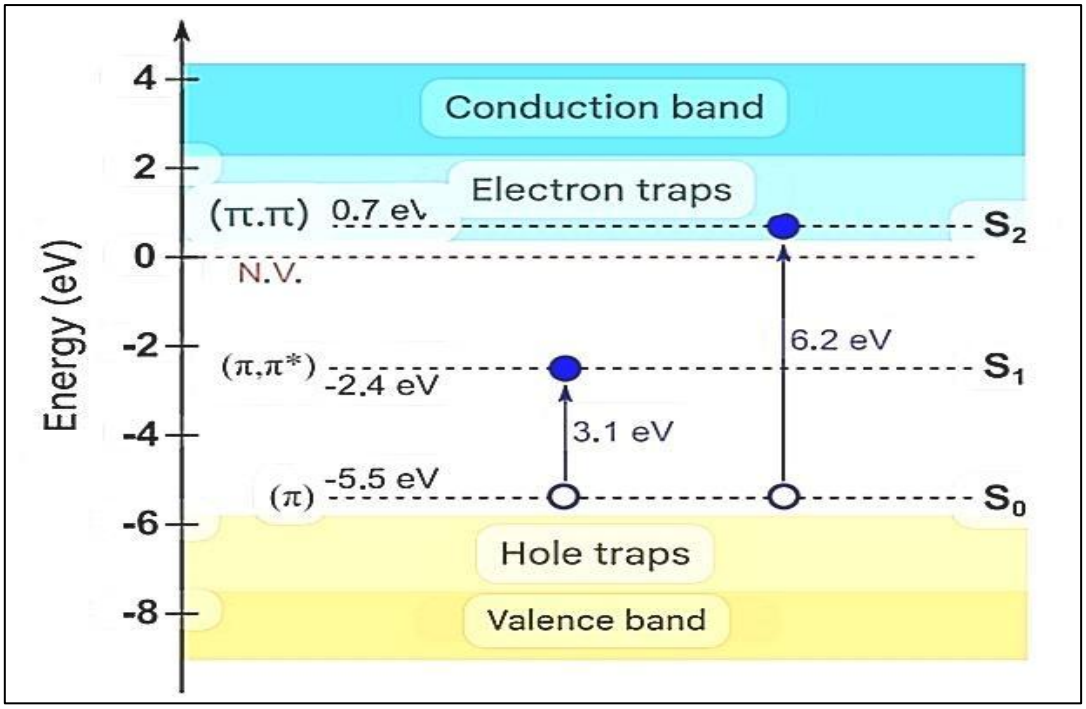

Figure 6. Schematic representation of the energy levels of the BOPP film and the electronic transitions responsible for optical absorption.

The PSD current peaks observed at energies of 3.1 eV and 3.3 eV (S1) appear not to be directly attributable to carrier photoemission from the irradiated electrode ,This is because the height of the potential barrier for electron injection, determined by the polymer characteristics and equivalent to 4.8 eV (representing the energy difference between the Fermi level and the LUMO level of polypropylene calculated by DFT), exceeds the energy of these peaks. In this context, the barrier height agrees with the current peak observed at 4.8 eV in the ITO-coated sample, as well as with the inflection point of the current increase associated with the peak at 5.9 eV. It is therefore plausible that these two peaks are related to photoinjection, although the maximum value of the higher-energy peak does not perfectly coincide with the barrier height. (Nguyen, H. V. *et al*., 2018)

The peaks associated with the S1 exciton could have at least two distinct origins. The first hypothesis envisages the release of an electron via the Auger effect. According to this scenario, the formation of an exciton from the SO level and with an energy between 3.1 eV and 3.3 eV would generate a hole which, once filled, would induce sufficient energy to trigger the release of a charge. The second possibility considers the radiative relaxation of this excited charge.

Photo-induced phenomena, such as the photoluminescence observed in polypropylene (PP), are closely associated with unsaturation. inherent to polyenones, polar sequences that often constitute sites conducive to the formation of deep traps favoring recombination processes.

The fluorescence emission, detected at an energy of 3.8 eV, is attributed to the presence of unsaturated carbonyls of the enone type, while the phosphorescence emission, located between 2.5 eV and 2.8 eV, is directly linked to the presence of unsaturated carbonyls of the di-enone type ,Optical excitation in the energy range of 3.1 eV to 3.3 eV can therefore indirectly lead to the release of charges trapped within localized states The energy absorbed by the material can cause the formation of excitons, which, during their relaxation, can generate a thermal vibration through an internal conversion, subsequently leading to the emission of phosphorescence. This thermal vibration could transfer energy to the trapped charges, giving rise to the PSD current, while radiative recombination would be at the origin of the light-induced recombination (LIR) luminescence spectra, as shown in Figure 7, with an emission peak located at 2.5 eV.

Publisher: SARC Publisher

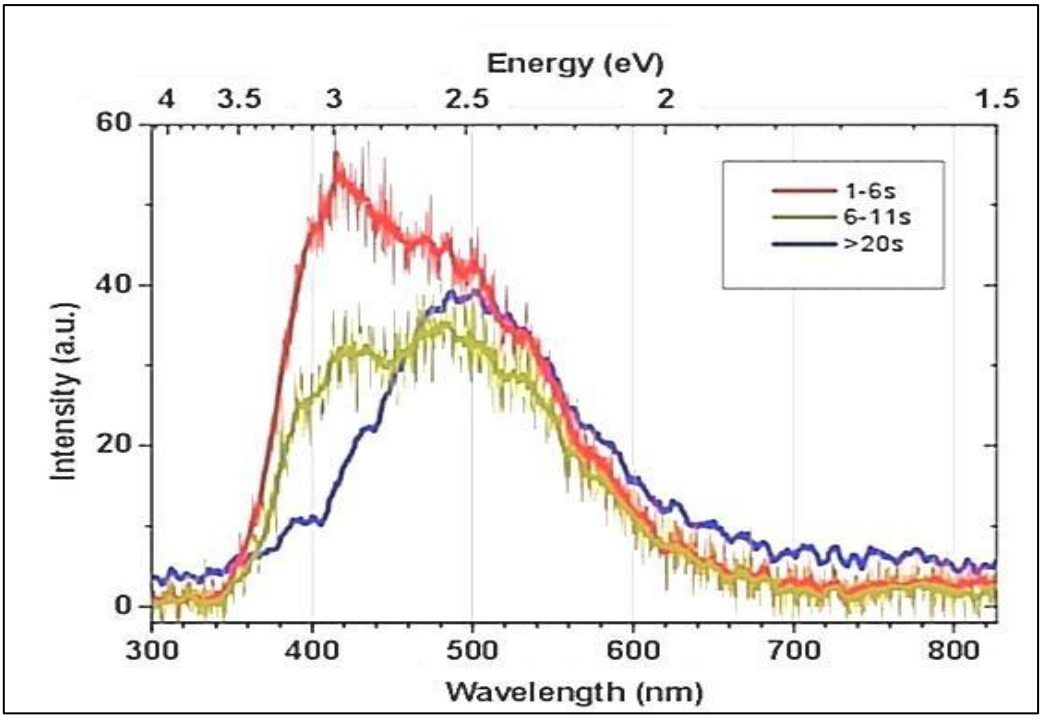

Figure 7. Plasma-Induced Luminescence (PIL) spectra. In the short term (red and khaki curves), the light emission may result from chemiluminescence and/or phosphorescence induced by the UV rays of the discharge. In the long term (blue curve), the response is considered representative of radiative recombination of the PIL charges .

Both dynamics mentioned may be amplified by the considerable photon flux density from the light source, lying in the same energy band.

Indeed, the inflection point observed in the increase in the PSD photodischarge current coincides with the global maximum flux density, which is found at 2.6 eV, while the current peak correlates with a local maximum flux at 3.1 eV. High photon flux, combined with a region of low light absorption, may contribute toexplain the relatively low current peak by increasing the probability of exciton generation. (Suraci, S. V. *et al*., 2023).

The current peak with both the largest amplitude and the broadest spectral width (5.9 eV) corresponds significantly to the most pronounced absorption band in the BOPP film.

Consequently, this photoinduced current can be associated with entities that, in theory, absorb in the energy range between 5 eV and 6.5 eV. These entities include additives such as antioxidants, carbonyl defects, or diene formations. On the one hand, it has been shown that most chemical defects, such as C-C double bonds, carbonyl groups, and dienes, possess well-defined electronic structures with band transition energies above 5.5 eV.

On the other hand, the antioxidant Irganox 1010, an aromatic compound whose chromophore is the phenyl group, is responsible for the absorption band of BOPP, with a peak at 6.2 eV (as shown in Figure 4 (a)). It appears to be the source of deep trapping sites, as has been studied with different phenolic antioxidants It is noteworthy that Irganox 1010 has a band gap of 5.4 eV This value could correspond to the creation of excitons by a band-band transition, which coincides with the energy of the PSD current peak. Once the S2 excitons are generated, they can be dissociated by the local electric field due to their weak binding.

The relationship between the PSD current peak at 5.9 eV and the mentioned chromophores is also validated by the absence of the high-energy current peak when the insulator is covered with a layer of ITO. This is because the transparent conductive material prevents the transmission of light with an energy higher than 5 eV, thus hindering the interaction of photons with chemical defects or the antioxidant, and, consequently, inhibiting the creation of excitons capable of generating a current in the external circuit Taking into account the PSD current peaks at 3.1 eV and 5.9 eV identified in the films studied, as well as additional information relating to the Auger effect of the S1 exciton and the electronic transition of Irganox 1010 associated

Publisher: SARC Publisher

with the S2 exciton, we are able to present the energy diagram illustrated in Figure 8.

This diagram highlights the mechanisms underlying the creation of free charges linked to PSD photodischarge currents in BOPP.

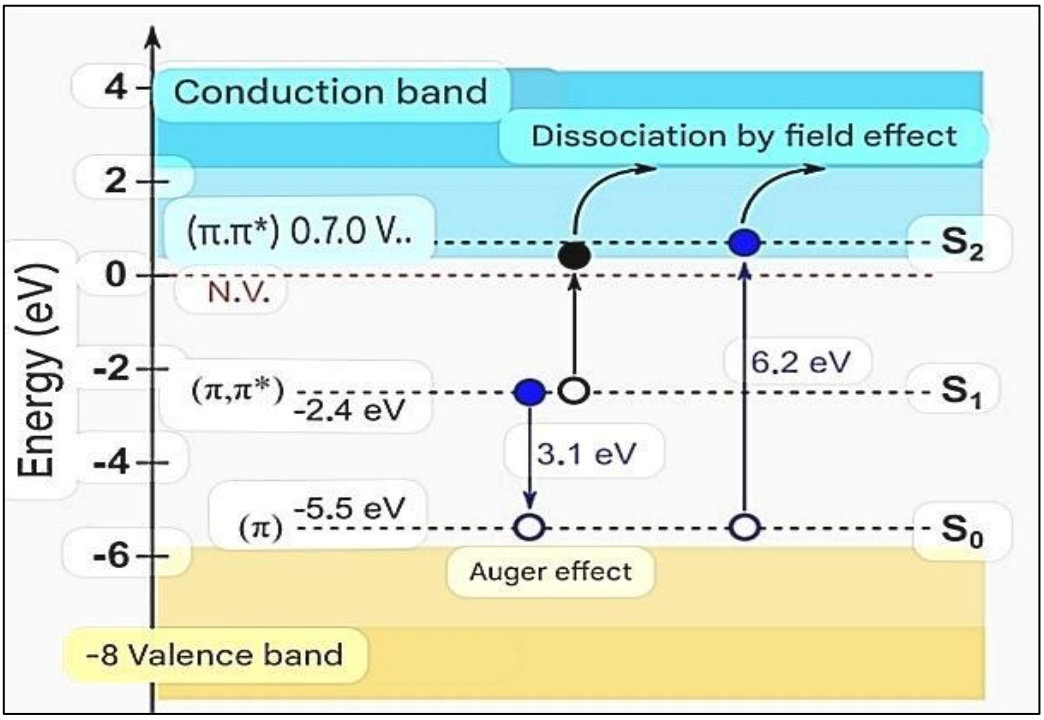

Figure 8. Schematic representation of the electronic transitions of the BOPP film explaining the creation of free charges during PSD irradiation

The results of photostimulated current (PSD) measurements revealed higher current peaks in the presence of positive space charge near the top electrode compared to the opposite polarity ,These observations suggest that the photostimulated current is influenced by the space charge distribution, favoring charge flow in one direction over the other.

Figure 9(a) shows an energy diagram of the metal-insulator contact after being positively charged and when exposed to light irradiation.

During the positive voltage charging period, the presence of positive space charges generates an upward curvature of the energy bands due to the electric field created between the insulator and the conductor, thus creating a zone called a depletion layer ,This phenomenon, commonly studied in the field of semiconductors, is known as band bending In response to UV irradiation, the polymer is able to absorb incident photons, thus inducing the formation of excitons near its surface. These electron-hole pairs, once created, seek to dissociate into free charge carriers, and they attempt to diffuse through the polymer. The holes can be transferred through the HOMO level of the polymer and collected by the metal electrode, thanks to the distortion of the electric field. The electrons generated by the effect of light can eventually be trapped, either in deep or shallow traps, or they can overcome these obstacles and move under the influence of the local electric field to be trapped in the volume or contribute to the electric current. On the other hand, in the case of the formation of a negative space charge (which, inthis study produces a deeper accumulation zone), the charges induce a downward bending of the bands and the creation of an accumulation zone, as illustrated in Figure 9 (b).

The generated excitons are theoretically less likely to dissociate or contribute to current flow, because conduction sites are not available, either in the bulk of the material or at the interface, for either charge carrier.

Publisher: SARC Publisher

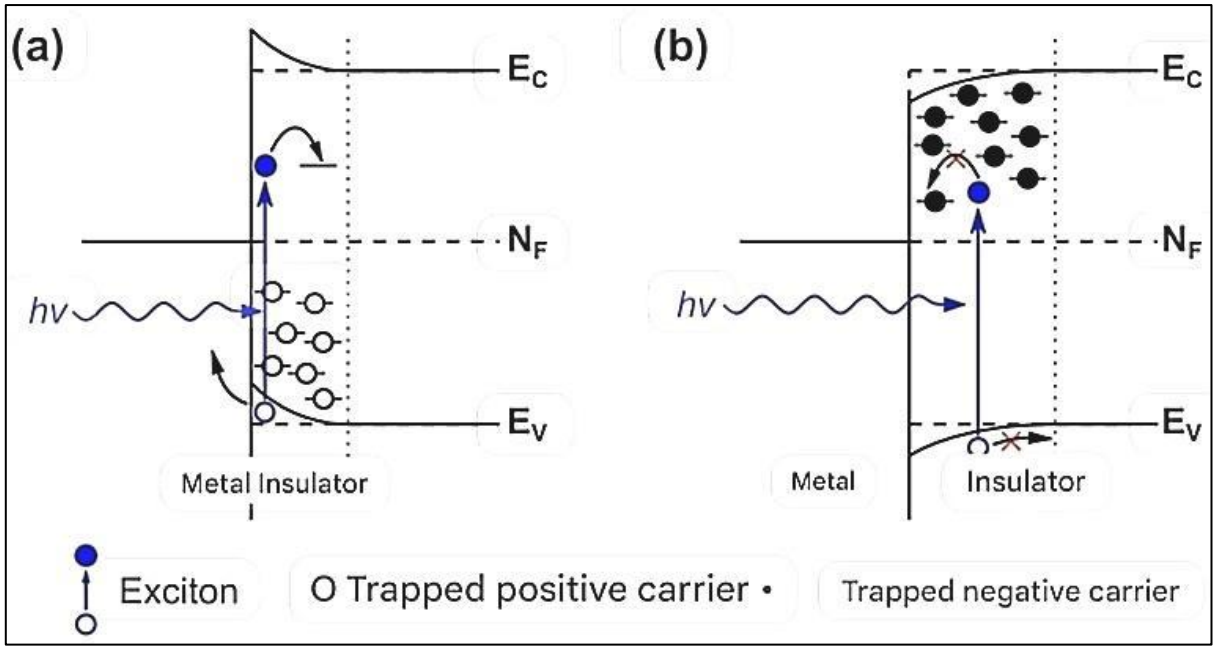

Figure 9. Schematic diagrams of the metal-insulator contact when irradiated by light. The positive space charge can allow greater dissociation of excitons (a) compared to a negative space charge (b).

CONCLUSION

Analysis of photoinduced currents and their correlation with absorption spectra reveal the ability to identify various entities foreign to the polymer chains, influencing charge trapping and detraining processes. The BOPP films examined mainly show two light excitation bands in the UV-visible spectral range , The S1 excitons, generated with energies around 3.1 eV, are potentially associated with transition metal ions, likely to generate free charges through the Auger effect or after producing undissipated energy through luminescence.

The highly energetic photons, located around 6.2 eV, could be attributed mainly to the creation of S2 excitons, whose nature is closely linked to chemical additives, such as phenolic antioxidants. These high-energy transitions could easily release electrons under the effect of the residual field associated with the charge present in space. Despite the absence of identifiable alterations in the sample's charge density following PSD irradiations, including scans and constant-energy excitations, the results obtained provide us with the opportunity to identify chromophoric species closely associated with the trapping characteristics inherent in BOPP.

Exploring different types of polymer materials, nonpolar in nature and possessing light-absorbing constituent structures, could contribute to a better understanding of the mechanisms underlying the trapping and release of electrical charges in polymer materials.

REFERENCE

1. Mayerhöfer, T. G., Pahlow, S., & Popp, J. "The Bouguer-Beer-Lambert law: Shining light on the obscure." *ChemPhysChem* 21.18 (2020): 2029-2046.
2. Xu, R., Xing, J., Du, B., Xiao, M., & Li, J. "Improved breakdown strength of polypropylene film by polycyclic compounds addition for power capacitors." *Materials* 14.5 (2021): 1185.
3. Takada, T., Ren, H., Li, J., Wang, W., Chen, X., & Li, Q. "Application examples of quantum chemical calculation." *Electric Charge Accumulation in Dielectrics: Measurement and Analysis*. Singapore: Springer Nature Singapore, (2022). 243-294.
4. Liu, H., Du, B. X., Xiao, M., & Tanaka, T. "High-temperature performance of dielectric breakdown in BOPP capacitor film based on surface grafting." *IEEE Transactions on Dielectrics and Electrical Insulation* 28.4 (2021): 1264-1272.
5. Yuan, M., Zhang, G., Li, B., Chung, T. M., Rajagopalan, R., & Lanagan, M. T. "Thermally stable low-loss polymer dielectrics enabled by attaching cross-linkable antioxidant to polypropylene." *ACS applied materials & interfaces* 12.12 (2020): 14154-14164.
6. Yuryevna Ridzel, O., Kalbe, H., Astašauskas, V., Kuksa, P., Bellissimo, A., & Werner, W. S.

Publisher: SARC Publisher

"Optical constants of organic insulators in the UV range extracted from reflection electron energy loss spectra." *Surface and Interface Analysis* 54.5 (2022): 487-500.

7. Ran, Z. Y., Du, B. X., Xiao, M., Liu, H. L., & Xing, J. W. "Dielectric property improvement of polypropylene films doped with POSS for HVDC polymer film capacitors." *IEEE Transactions on Dielectrics and Electrical Insulation* 28.4 (2021): 1308-1316.
8. Ohki, Y., Fuse, N., & Arai, T. "Band gap energies and localized states in several insulating polymers estimated by optical measurements." *2010 Annual Report Conference on Electrical Insulation and Dielectic Phenomena*. IEEE, (2010)
9. Uehara, H., Okamoto, T., Sekii, Y., Iwata, S., & Takada, T. "Analysis of charge trap depth using Q (t) method and quantum chemical calculation in XLPE and PE with phenolic antioxidant." *2021 IEEE Conference on Electrical Insulation and Dielectric Phenomena (CEIDP)*. IEEE, (2021).
10. Teyssedre, G., Mendoza-Lopez, D., Laurent, C., Boudou, L., Berquez, L., & Zheng, F. "Charge trap spectroscopies in polymer dielectrics: application to BOPP." *2021 3rd International Conference on High Voltage Engineering and Power Systems (ICHVEPS)*. IEEE, (2021)
11. Nguyen, H. V., & Pham, T. H. "Structural and Electronic Properties of Defect-Free and Defect-Containing Polypropylene: A Computational Study by van der Waals Density-Functional Method." *physica status solidi (b)* 255.3 (2018): 1700036.
12. Suraci, S. V., Mariani, D., & Fabiani, D. "Impact of antioxidants on DC and AC electrical properties of XLPE-based insulation systems." *IEEE Access* 11 (2023): 76132-76141.

Source of support: Nil; **Conflict of interest:** Nil.

Cite this article as:

Hussein, A. F. "Study of Charge Trapping and De-Trapping Phenomena through Vacuum Charge Measurements and Photoinduced Discharge in Polymeric Thin Films for Energy Storage" *Sarcouncil Journal of Engineering and Computer Sciences* 4.9 (2025): pp 196-208.

Publisher: SARC Publisher